Polyvinylidene Fluoride Hollow Fiber Membranes for Refinery Wastewater Treatment: Effect of Air Gap Length on Membrane Morphology and Performance

By Amrifan Saladin Mohruni

WORD COUNT 6255 TIME SUBMITTED 12-APR-2023 11:50PM

PAPER ID 98652464

Polyvinylidene fluoride hollow fiber membranes for refinery wastewater treatment: Effect of air gap length on membrane morphology and performance

E. Yuliwati[a,*], A.F. Ismail[b,c] A.S. Mohruni[d], T. Matsuura[b,e]

[a]*Department of Industrial Engineering, Faculty of Engineering, University of Bina Darma, Sumatera Selatan, Indonesia*
Tel. +62 (711) 515-679
[b]*Advanced Membrane Technology Research Centre (AMTEC),*
[c]*Faculty of Petroleum and Renewable Energy Engineering, Universiti Teknologi Malaysia, 81310 UTM, Skudai Johor, Malaysia*
Tel. +60 (7) 553-5592; Fax: +60 (7) 558-1463
[d]*Department of Mechanical Engineering, Faculty of Engineering, Sriwijaya University, Sumatera Selatan, Indonesia*
Tel. +62 (711) 580-272
[e]*Department of Chemical Engineering, Industrial Membrane Research Laboratory, University of Ottawa, Ont., Canada KIN 6N5*

Corresponding author: **erna_yuliwati@mail.binadarma.ac.id*

Abstract

Effects of air gap length on outer surface morphology and filtration performance of hydrophilic polyvinylidene fluoride (PVDF) hollow fiber membrane have been studied. Porous asymmetric hydrophilic PVDF membranes were prepared via a phase inversion method, using N,N-dimethylacetamide (DMAc) as solvent, lithium chloride monohydrate ($LiCl.H_2O$) and titanium dioxide (TiO_2) as inorganic additives. Submerged membrane ultrafiltration was conducted using non-ionic solutes of different molecular weight and refinery wastewater with constant suspended solid concentration. The comparison of the performance and morphology was conducted between PVDF membranes of different air gap length at 1, 4, 11, and 15 cm. The prepared membranes were characterizedthrough observations of field emission scanning electron microscope (FESEM) and atomic force microscopy (AFM), permeate flux measurement, and tensile propertytest.Average pore size and surface porosity were calculated by the permeate flux in submerged membrane system. It is resulted that the permeate flux is mainly determined by effective porosity.Moreover, the average pore size and nodules size were increased, while outer surface membrane was being smoother with increasing of air gap length. AFM analysis reveals that the air gap introduces an elongation stress due to the gravity on the membrane surface. Under the air gap length of 11 cm high permeate flux of 148.53 L/m^2h and suspended solids removal of 99.82 % and also relatively high mechanical strength of membrane can be simultaneously achieved. It is concluded that there exists the best range of the air gap length for relatively high performance of membrane.

Keywords: air gap length; roughness; pore size; porosity; flux.

1. Introduction

Synthetic membrane technology has grown up very fast and has received significant attention from both academia and industry, since the first mention of hollow fiber membranes in a series of patents by Mahon in 1966 and 1966b [1,2]. Nowadays, the hollow fiber membrane configuration via phase inversion process is the most favored membrane geometry in the most membrane applications. Hollow fibers have much larger surface area per unit volume of the membrane module and hence offer higher productivity per unit volume. They have also good flexibility in operation [3,4].

However, during membrane formation, the preparation of the hollow fibers often requires more controlling parameters than those of flat sheet membranes (i.e. structure and dimensions of the spinneret, viscosity and possibility of the spinning dope, nature of the internal and external coagulants, flow rate of the bore fluid, dope extrusion rate, air gap length, take-up speed, etc) [5]. Among the studies of membrane formation by the dry-jet wet spinning process, the effects of air gap length on final hollow fiber membrane have been investigated by many researchers [6-9]. However, the fabrication of a hollow fiber with desirable performance is not trivial process and the effect on hollow fiber membrane morphology and permeation process reported in the literatures often provide conflicting observations. For instance, in spinning polysulfone hollow fibers, Aptel *et al.*, (1985) reported that the permeability decreased as the air gap length increased [10]. On the other hand, it was reported by Kim *et al.*, (1995) that air gap length had no impact on the permselection properties of polysulfone hollow fibers [11]. Khayet (2003) was also investigatedthat the separation factors of polyvinylidene fluoride hollow fibers increases with increasing the air gap distance; however, the air gap distance did not significantly affect the permeation rate [12]. He attributed this fact to the increase of the skin layer thickness with increasing the air gap length. In addition, air gap length also proved to be an easy and powerful tool to tune the prem-selective properties of hollow fiber membranes during spinning process.It has been also reported that the membrane spun from air gap length of 20-30 cm exhibited very poor permeability, higher value of permeability were obtained from air gap length of 10-15 cm and for lower air gap length the permeability was reduced drastically [13]. Tsai *et al.* (2002)

observed that the both inner and outer diameters decreased with increase of the air gap distance. It was reported that the elongation stress due to gravity anneals the fiber caused the change of inner and outer diameter [14]. Khulbe *et al*. (2004) and Khayet *et al*. (2009) have similar results when using polyetherimide (PEI) polymer and polyvinylchloride (PVC) polymer respectively [15,16]. It was explained that stress inside the spinneret perpendicular to the fiber axis released when dope solution comes out from spinneret. This will expand the fiber diameter, whereas the stress parallel to the fibers will elongate the fiber and diminishing its diameter.

In this study, air gap length plays an essential role in the PVDF ultrafiltration membrane preparation,meanwhile, all parameters were kept constant.The objective of this study is to investigate the effects of air gap length on the morphological structure and filtration efficiency of hydrophilic polyvinylidene fluoride (PVDF) membrane. Four varied air gap lengthsof 1,4,7,and 15 cm wereused in order to produce different structure and morphology of membrane. Based on this results obtained, it is expected to find out the suitable PVDF membrane for preparation of hydrophilic ultrafiltration membrane for refinery produced wastewater treatment.

2. Experimental

2.1. Materials

Ultrafiltration membranes have been prepared using Kynar®740 PVDF polymer pellets were purchased from Arkema Inc. Philadelphia, USA. The solvent N,N-dimethylacetamide (DMAc, Aldrich Chemical) (Synthesis Grade, Merck, >99%) was used as polymer solvent without further purification. Lithium chloride monohydrate ($LiCl.H_2O$) and nanoparticles titanium dioxide (TiO_2) were used as inorganic additives. Both chemical additives were purchased from Sigma-Aldrich and used as received. Glycerol was purchased from MERCK (Germany) and used as non-solvent for post treatment of membrane. In all cases, tap water was used as the external coagulation bath medium in the spinning process.

2.2. Preparation of spinning dopes

An amount of pre-dried (24 h oven dried at 50°C) PVDF pellets in ranging of 16 to 22 wt.%were weighed and poured into pre-weighed DMAc solvent. The mixtures were stirred to ensure thorough wetting of polymer pellets, prior to the addition of appropriate amounts of $LiCl.H_2O$ at 50 °C. TiO_2 was then carefully added to the polymer dope mixtures, which were continuously stirred for 48 h (IKA-20-W) at 500 rpm until a homogenous solution was formed. The polymer solution was kept in a glass bottle and air bubbles formed in the dope were removed using water aspirator for several hours.The fully dissolved polymer solution was transferred to a glass reservoir, allowed to stand and degassed for 24 h at room temperature prior to spinning process. Solution viscosity was measured using rheometer (Bohlin Instrument Ltd.) at various temperatures between 25 and 50 °C.

2.3. Fabrication of hollow fiber membranes

2.3.1 Spinning parameters

In this study, hollow fiber membrane is produced through a dry-jet wet spinning process. The membrane can be formed only in the appropriate conditions of all the spinning parameters (i.e. dope extrusion rate, extrusion velocity from spinneret, take up speed, bore fluid rate, and air gap length). The air gap length variable in the spinning system effects the fiber geometry in terms of the inner diameter, outer diameter, wall thickness, and structure of membrane sublayer. This may be attributed to the die swell of polymer macromolecules when exiting from the spinneret due to the viscoelastic properties of the PVDF spinnning dope. Furthermore, the gravity will influence the achievable in the spin line and introduces an elongation stress on membrane and generally tends to decrease the membranes wall thickness.

2.3.2 Dry-jet wet spinnning process

PVDF hollow fiber UF membranes were spun at room temperature by a dry-jet wet spinning method. The spinning solutions were consisted of maintained PVDF concentration of 19 wt.%, which were prepared at different air gap lengthof 1, 4, 11, and 15 cm. $LiCl.H_2O$ and

TiO_2 were maintained at 5.2 wt % and 10 wt.% of the weight of PVDF, as shown in Table 1 respectively. The hollow fiber spinning process by dry-jet wet phase inversion was explained by Qin*et al.*,(2001); Ismail and Hassan (2006) [17,18]. The detailed spinning parameters are listed in Table 1.

Table 1 Spinning conditions of the hollow fiber membranes

Spinning condition	Value
Dope extrusion rate (ml/min)	4.20
Bore fluid	Distilled water
Bore fluid flow rate (ml/min)	1.40
External coagulant	Tap water
Air gap distance (cm)	1, 4, 11, 15
Spinneret od/id (mm)	1.10/0.55
Coagulation temperature ˚C	25
Room relative humidity (%)	70 – 75

The hollow fiber membranes were produced using the dope formulation solution composed of PVDF/LiCl.H_2O/TiO_2 at different polymer concentration, as shown in Table 2.

Table 2.The air gap length condition for holow fiber membrane preparation

Membrane	PVDF concentration, wt.%	PVDF/LiCl.H_2O/TiO_2ratio in DMAc	Air gap length, cm
PTL-19-1	19	19/0.98/1.95	1
PTL-19-4	19	19/0.98/1.95	4
PTL-19-11	19	19/0.98/1.95	11
PTL-19-15	19	19/0.98/1.95	15

2.3.3 Post-treatment

The spun fibers were cut in pieces of approximately 50 cm in length and then stored in water bath at room temperature for at 1 day to remove the residual solvent. The fibers were then soaked in the 20 wt.% glycerol aqueous solution bath for another 1 day in order to prevent pore collapse or change of transport properties during drying at room temperature for 4 days, they were ready for making hollow fiber test bundles as mentioned in our previous study by Yuliwati and Ismail (2011) and Yuliwati et al., (2011) [16,17}.

2.4 Filtration experiments

The permeation flux and rejection of PVDF hollow fiber membranes for synthetized refinery wastewater were measured by submerged ultrafiltration experimental equipment as shown in Fig.1 [16]. An in-house produced U-shape hollow fiber module, with a filtration area of 11.23 dm^2, was submerged in prepared suspension in membrane reservoir with volume of 14 L. A cross-flow stream was produced by air bubbling generated by a diffuser situated underneath the submerged membrane module for mechanical cleaning of the membrane module. The air bubbling flow rates per unit projection membrane area was set constantly at 2.4mL/min in order to maintain proper turbulence. The filtration pressure was supplied by a vacuum pump and controlled by a needle valve. Permeate flow rates were continually recorded using flow meter respectively.

In order to conduct the studies at steady state, the hollow fiber membranes have to compacted at a transmembrane pressure (TMP) of vacuum. The desired TMP was controlled using the pressure regulator installed at the outlet of the membrane reservoir. TMP is the driving force for the pressure-driven membrane process and is defined as the pressure difference across the membrane,

$$\mathrm{TMP} = \left[\frac{P_f + P_r}{2}\right] - P_P \qquad (1)$$

where P_f is the feed pressure (bar), P_r is the retentate pressure (bar), and P_P is the permeate pressure (bar).

Membrane performance was tested with anin-house U-shape membrane bundle having about 11.23dm^2 of membrane surface area. Pure water flux was measured after the flux was steady. The collected permeate can be recorded in terms of flux and rejection by the expression as follows,

$$J_w = \frac{V}{At} \qquad (2)$$

where J_w is the pure water flux (L/m^2 h), V is the permeate volume (m^3), A is the membrane surface area (m^2), and t is the time to obtain the quantity (s).

The values of J_w obtained from the experiments were converted to corresponding unit of m.s^{-1} during data analysis for better understanding. The pure water permeability coefficient, L_p was then determined from the values of J_w versus the applied pressure for all the studied membranes with the assumption of null value of the osmotic pressure, π.

$$J_w = L_p . \Delta P \quad (3)$$

The second property of feed contained neutral solute-PEG with different MWs at a concentration of 200 ppm. This feed solution was used for the characterization of MWCO of a membrane. The solute rejection was determined based on the total organic carbon (TOC) rejection determined by total organic carbon analyzer, TOC-$V_{CSH/CSN}$ (Shimadzu Corporation). The third property of feed contained synthetic refinery wastewater at constant concentration that based on mixed liquor suspended solids (MLSS) concentration of 3 g/L. The conductivity of refinery wastewater for the feed and permeate was measured using conductivity meter (EC300, YSI Inc.). In order to determine the rejection, the effective solute filtration efficiency, R (%) can be calculated using the following equation:

$$R = \left(1 - \frac{C_p}{C_f}\right) x\ 100 \quad (4)$$

Where R is the rejection ultrafiltration process (%), C_p is the concentration of the permeate (mg/L) and C_f is the concentration of the feed (mg/L).

2.6. Characterizations

The morphological structures of the hollow fiber membranes were studied using field emission scanning electron microscope (JEOL JSM-6701F). The FESEM micrographs of the cross section membranes were taken at certain magnifications. It produced photographs at the analytical working distance of 10 nm.

Atomic force microscopy (AFM) was used to study the external and internal surfaces of the prepared PVDF hollow fiber membranes. The AFM images were obtained over different areas of each hollow fiber membrane using a tapping mode Nanoscope III equipped with 1553D scanner (SPA-300 HV,USA). In this study, scans were made on areas of 5 μm × 5 μm. The AFM analysis software program allowed computation of various statistic related to the surface roughness on predetermined scanned membrane area. To determine the pore sizes and nodule sizes, cross-sectional line profiles were selected to traverse the obtained AFM images and the diameter of nodules (i.e. high peaks) or pores (i.e. low valleys) were measured by means of a pair of cursors. The sizes of the nodule aggregate are based on the average of 15 measurements.In terms of surface roughness, the outer surface of the PVDF hollow fiber membranes were compared using various roughness parameters such as the mean roughness (R_a), the root mean-square roughness (R_q) and the average difference in height between the five highest peaks anf the five lowest valleys (R_z) [16,19]. The average pore sizes and average nodule sizes of outer surfaces were also determined. Those were measured, as stated previously, by inspecting line profiles on the AFM images at different locations of a membrane surface. The measured pore sizes from the line profiles on the AFM micrographs were arranged in ascending order and the median rank (50%), χ, was calculated using the followed equation,

$$\chi = \left(\frac{i - 0.3}{n + 0.4} \right) 100 \qquad (5)$$

where i is the order number of the measured pore size arranged in ascending order and n is the total number of the measured pores.

Differences in the membrane surface morphology can be expressed in terms of various roughness parameters, such as (1) the differences between the highest and the lowest points

within the given area, *Z;* (2) the root mean-square of the *Z* data within the given area (R_{RMS}); (3) the mean roughness (R_a). This parameter represents the mean value of the surface relative to the centre plane, the plane for which the volume enclosed by the image above and below this plane is equal. It is calculated as follows

$$R_a = \frac{1}{L_x L_y} \int_0^{L_x} \int_0^{L_y} |f(x,y)| dxdy \qquad (6)$$

where $f(x,y)$ is the surface relative to the centre plane, L_x and L_y are the dimensions of the surface in the x and y directions, respectively; (4) the average difference in height, R_z, between five highest peaks and five lowest valleys is calculated relative to the mean plane, which a plane has a data variance. Roughness parameters obtained from AFM micrographs should not be considered as absolute values because it depends on the treatment of the captured surface data such as plane fitting, flattering, filtering, etc. In the present study, the same tip was used for all experiments and all captured surfaces were treated in the same method. The evaluation of the roughness parameters of each sample was based on micron scan areas. Porosity was calculated also by the method described by Singh *et al*. (2008) [19].

Asymmetric porous membranes were characterized by determination of porosity and average pore radius. The membrane porosity, ε,was defined as the volume of the pores divided by the total volume of the porous membrane. The membrane porosity was calculated using the following equation,

$$\varepsilon = \frac{\frac{(w_1 - w_2)}{\rho_W}}{\frac{(w_1 - w_2)}{\rho_W} + \frac{w_2}{\rho_P}} \times 100 \qquad (7)$$

where ε is the porosity of the membrane (%), w_1 the weight of wet membrane (g), w_2 the weight of dry membrane (g), ρ_p the density of the polymer (g/cm^3) and ρ_w is the density of water (g/cm^3).

To prepare the wet and dry membranes, five spun hollow fibers with the length of 25 cm were selected after solvent was exchanged in tap water for 3 days. The fibers were immersed into

the isopropanol for 3 days and distilled water for 3 days. The remained water in the inner surface was removed using air flow, before weighing the membranes. The wet membranes were dried in vacuum oven for 12 h at 40 °C and weighted.

Average pore radius, r_m, was investigated by filtration velocity method, which a measurement of the ultrafiltration flux of the wet membrane applied on pure water in limited time (20 h) under 0.1 MPa pressure. It represents the average pore size along the membrane thickness (ℓ), which was measured by the difference value between external radius and internal radius of the hollow fiber membrane. The test module containing 60 fibers with the length of 35 cm was used to determine water permeability. According to Guerout-Elford-Ferry Equation, r_m could be calculated:

$$r_m = \sqrt{\frac{(2.9-1.75\varepsilon)\,x\,8\eta\ell Q}{\varepsilon\,xAx\,\Delta P}} \qquad (8)$$

whereη is water viscosity (8.9 x 10^{-4} Pa s), ℓ is the membrane thickness (m), ΔP is the operation pressure (0.1MPa), ε is the porosity of the membrane (%), Q is volume of permeate water per unit time ($m^3\ s^{-1}$), A is an effective area of membrane (m^2).

3 Result and discussion

3.1 Effect of PVDF concentration on the membrane structure and filtration performance

3.1.1 Morphology studies by FESEM and AFM

The morphology of the membraneswas studied by FESEM to represent the cross-sectional and surface at certain magnification.Heterogenous structure with top skin supported by finger-like macrovoids substructure was often observed in many types of hollow fiber fabricated via the phase inversion method due to the fast solvent and non-solvent exchange rate [20]. Figure 1 shows FESEM micrographs of the cross-sectional morphology of the prepared PVDF UF membranes. Increasing PVDF concentration in the range of 16 to 22 wt.% demonstrated an obvious change of morphology and suppressed both of inner and outer finger-like macrovoids.

The finger-like structure under the top layer, as this structure was prepared from 22 wt.% PVDF in Figure 1(c), was much less than membrane structure prepared from 19 wt.% PVDF in Figure 1(b). Furthermore, there was also a transition from macroporous structure to asymmetric structure in membrane cross-section. A more sponge-like substructure and thicker top layer of membranes were formed across the membrane wall. This can be explained by the fact that higher dope viscosity decreases the solvent (DMAc) and non-solvent (water from coagulation medium) exchange rate, thus resulted in higher resistance of diffusion from polymer aggregation. From FESEM images, pores had not been observed under FESEM at a magnification of 40.000. The results confirmed that the pores on the membrane surface were in range of nanometer. Based on the previous studies, it is reported that pore size decreases with increasing polymer concentration due to the increase in the solution viscosity, leading to a stronger molecular orientation and tighter structure [21,22]. Therefore, it is expected that membrane pores tend to be decreased with polymer concentration. To verify the result from FESEM images, membrane characterization by means of pure water measurement and solute tranport method were carried out in the following sections.

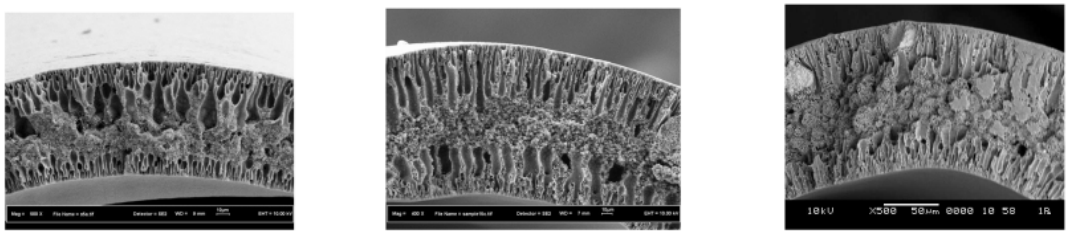

(a) (b) (c)

Fig.1. Partial cross-section of hollow fiber membranes (a) PVDF-16 (b) PVDF-19 (c) PVDF-22

3.1.2 Flux characteristic

Experiment were performed with distilled water to determine the pure water flux (PWF) and PWF coefficient of PVDF membranes prepared from different polymer concentration. The experiments were tested using submerged membrane system at vacuum and room temperature. Figure 2 shows the evaluation of permeate flux obtained in these experiments. A straight line correlation was obtained with reasonably high coefficient (R^2 = 0.8715-0.9876) while plotting

the membrane permeability on ordinate vs. trans-membrane pressure. The example of membrane permeation data and its PWP determination is shown in Fig.2.

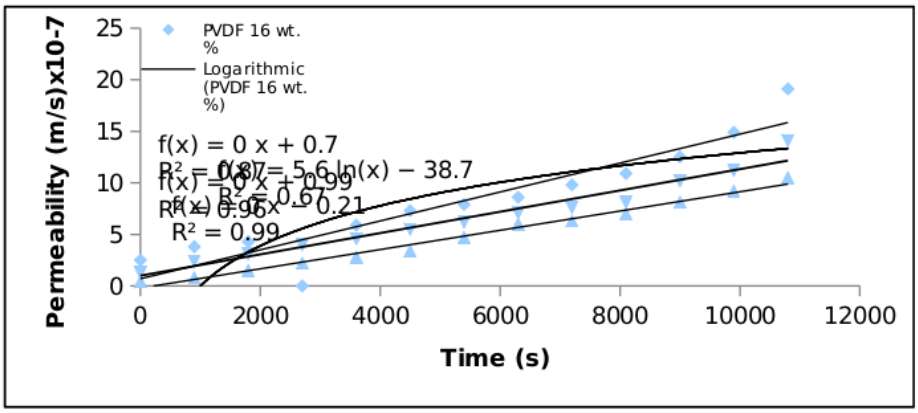

Fig.2. The pure water flux of the hollow fiber membranes prepared from 16 to 22 wt.% PVDF as a function of filtration time

3.1.2 Solute rejection characteristics

The filtration efficiencies of PVDF membranes were further demonstrated using two different feed solutions that based on suspended solids concentration (3000 mg/L and 4500 mg/L concentration) as shown in Figure 2. Basically, the electrostatic interactions between ions and membrane surface charge are responsible for ion filtration. Therefore, the steric-hindrance effect is also responsible for ion retentions. As can be seen in Figure 1, an increase in polymer concentration led to increase suspended solids removal efficiency. The results presented that increasing suspended solids removal is due to the corresponding decrease in average pore size of membranes as tabulated in Table 3.

Table 3 The PEG rejection and MWCO of various membranes as a function of PVDF concentration

[a]Membrane	Neutral solutes, R (%)				MWCO
	PVP k-30	PVP k-60	PVP k-90	PVP k-360	(kDa)
PVDF 16	19.20	36.70	48.45	60.30	77

	(±0.23)	(±0.07)	(±0.35)	(±0.03)	
PVDF 19	35.50 (±0.57)	78.86 (±0.21)	91.23 (±0.50)	98.83 (±0.04)	155
PVDF 22	30.20 (±1.01)	71.45 (±0.28)	82.45 (±0.09)	95.20 (±0.31)	185

[a]Test conditions : -15 in Hg, room temperature

Figure 4 shows the retention of suspended solids with different percentages of PVDF content based on suspended solids of 3.0 g/L and 4.5 g/L.

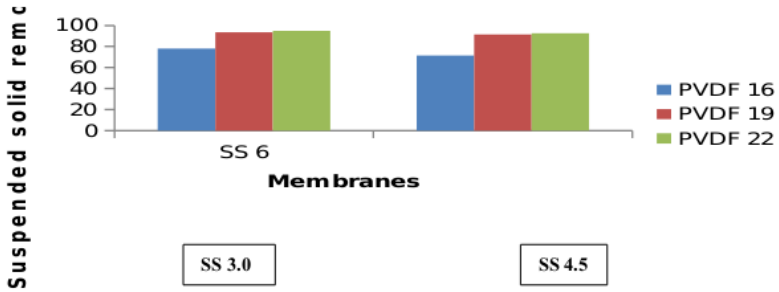

Figure 4: Suspended solids retention of hollow fibers prepared from 16 to 22 wt. %of PVDF

3.2 Effect of air gap length on the membrane structural and separation performance

It is well known that in hollow fiber spinning, the pressurized viscous solution is subjected to various stresses when it extrudes thorugh the complicated channel within a spinneret. These stresses may influence molecular orientation and relaxation, and subsequently fiber formation and separation performance, as well as productivity [23]. Macromolecules may experience swell and relax when exiting from spinneret, if there is an air gap before coagulation and will change their orientation.Figure 5 represents the AFM images of the surface properties of PVDF hollow fibers. These images revealed that the membrane surfaces were not smooth and that the nodule aggregates were formed at the surfaces of the PVDF hollow fibers. The mean roughness parameter R_a obtained from the AFM images showed 23.45, 15.02, 12.28, and 9.85 for the PTL-19-1, PTL-19-4, PTL-19-11, and PTL-19-15, respectively. The high peaks seen as bright regions in the AFM images characterize the nodules while the pores are seen as dark

depression. The figures further indicate that the surface nodule appears to be randomly arranged when the air gap is small but forms small rows of nodule aggregates aligned in the spinning direction for high air gap lengths. Generally, the average nodule size at the outer surface seems to increase with an increase of the air gap length. Molecular chains that experinced higher air gap tend to align themselves much better than those experienced lower air gap length; and this enhanced orientation will cause the polymer molecules to be packed closer to each other resulting in a tigher structure. The nodule size from the AFM images are listed in Table 4. Therefore, the average nodule size (nm) and standard deviation (S.D.) for air gap length of 1 cm larger than those of the other hollow fibers. This may be partly attributed to the fact that polymer macromolecules may experience die swell when existing from the spinneret as stated by Qin *et al.*, (2001) [24]. For the dry-jet wet spun fibers, 1 cm air gap length is not enough for molecular orientation induced by shear stress within the spinneret to relax in the air gap region. The average nodule size of hollow fibers increases clearly with increasing the air gap length (>4 cm). This may be due to the increase of interchain entanglement and the annealing of polymer chain with the air gap length. The radius of gyration and the collision frequency of polymer chains have also affected the nodule size on membrane surface.

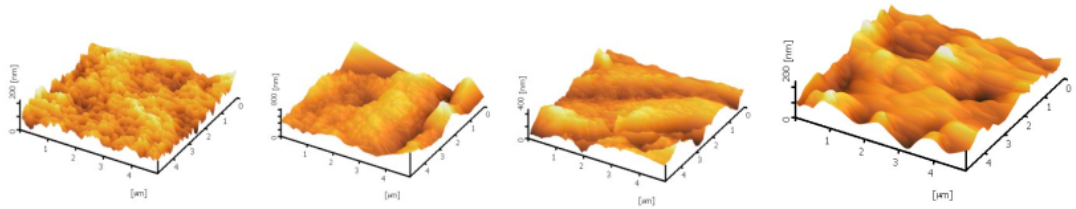

(a) (b) (c) (d)

Fig. 5. AFM images of outer surface hollow fiber membranes (a) PTL-19-1 (b) PTL-19-4 (c) PTL-10-11 (d) PTL-19-15.

Table 4. Results of the AFM analysis of the outer surfaces of PVDF hollow fiber membranes

Membrane	Nodule size		Roughness parameters		
	(nm)	S.D.	R_a (nm)	R_q (nm)	R_z (nm)
PTL-19-1	52.30	1.03	23.45	29.55	178.51
PTL-19-4	65.23	1.72	15.02	20.34	133.90
PTL-19-11	86.93	1.19	12.28	15.03	111.50

PTL-19-15	90.08	0.93	9.85	13.75	90.40

As can be seen from the table, it is noticed that the increase of air gap length impacted the higher values of pure water flux. Because the permeation flux is significantly influenced by the membrane thickness as given by the Hagen-Poisseuille equation, it is difficult to compare the permeability of different hollow fiber membrane thickness. In fact, the flux of the asymmetric membrane is governed bynthe thickness of the active surface layer and not by the total membrane thickness. Generally the skin layer thickness affects the membrane performances as well. The solvent evaporation rate and solvent/non-solvent exchange rate dominates the behaviour of skin layer formation during the dry-jet wet phase inversion procedures [25]. In the hollow fiber membrane formation process, the air gap length may be considered similar to the dry-jet wet phase inversion, resulting in the skin layer thickness inceases.

There was also a steady increase of the pore size of membranes with the change of air gap. At low air gap length, after existing from the spinneret, the fiber is immersed in the non-solvent coagulant bath almost rapidly than those at the higher air gap length. This results in a higher amount of the non-solvent and solvent trapped in the contracted polymer chains. Therefore, the fibers may have a longer random and less oriented polymeric chain interaction structure with intermolecular voids or free volume. It was mentioned above by Tsai et al., (2002) [25] that admitted the skin layer thickness increases with increasing the air gap length. Chung and Hu (1997) revealed that dry-jet wet spinning process resulted in external fiber skins with a compact and slightly oriented or stretched structure than the wet spun fibers [26]. They argued that there are two probably dominant mechanisms to induce molecular orientation during hollow fiber formation. Firstly, it is due to the elongation stresses (outside the spinneret) because the gravity and the second one is due to the shear and elongation stresses within the spinneret. In this study, it was observed that the PWP flux decreases when the air gap length is enhanced and the separation performance of a particular solte increases,. The caused is that PVDF fibers spun from a higher air gap length may have a greater orientation and tigher molecular packing than that at lower air gap length. Similar phenomenon has been discussed by Oh *et al.*,[27]. Chung *et al.*, (1999) [28], Hamid et al., (2010) [29], and [30]. They was suggested that an increase in an air

gap length might result in the selective layer with a greater orientation and tigher molecular packing.

It must be pointed out that when the air gap length was increased from 1 to 15 cm the PWP flux decreased by 43.65% but the filtration performance for a particular solute increases with increasing the air gap length. The results indicated that the pore size in outer and/or inner surface fibers may decrease with increasing air gap height becaused smaller pore size of the membranes and higher porosity resulting in better rejection for a solute solution and higher resistance for water/wastewater permeation, as illustrated curves in Figs. 6 and 7. The porosity increase by 30 % and the suspended solids concentration in the permeate decreased by 53.70 %.

Table 5. Properties of prepared PVDF hollow fiber membranes at different air gap lengths

Membrane	Air gap length (cm)	r_m (nm)	Wall thickness (mm)	PWP (L/m^2h)	PVP k-30	PVP k-60	PVP k-90	PVP k-360
PTL-19-1	1	40.32 (±0.05)	0.190 (±0.13)	121.25 (±0.15)	11.25 (±0.23)	23.45 (±0.07)	36.79 (±0.35)	58.88 (±0.03)
PTL-19-4	4	38.51 (±0.73)	0.185 (±0.05)	94.34 (±1.23)	25.71 (±0.23)	52.76 (±0.07)	75.50 (±0.35)	79.41 (±0.03)
PTL-19-11	11	34.05 (±1.01)	0.175 (±0.09)	82.50 (±0.07)	35.50 (±0.23)	78.86 (±0.07)	91.23 (±0.35)	98.83 (±0.03)
PTL-19-15	15	33.10 (±1.56)	0.170 (±1.01)	81.01 (±1.88)	38.01 (±0.23)	80.20 (±0.07)	93.48 (±0.35)	99.38 (±0.03)

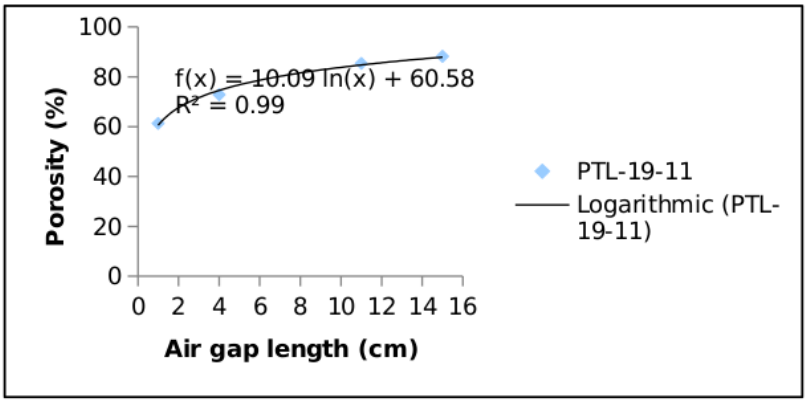

Fig. 6. Porosity of membranes versus air gap

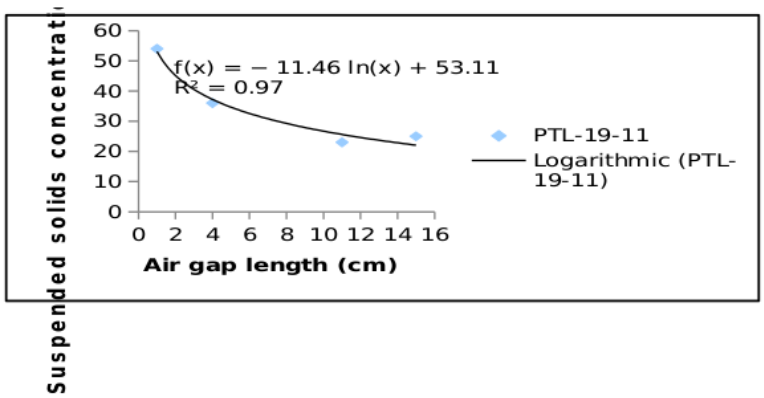

Fig. 7. Suspended solids concentration on the outer surface versus air gap

4 Conclusions

Based on the experimental results obtained, it is described that the membrane structure and performance are strongly dependent on the polymer concentration and air gap length. These observations have led to the conclusions, that the increase in polymer concentration in the spinning dope suppressed the formation of macrovoids in membrane substructure and resulted in denser skin layer. The change of finger-like to sponge-like substructure of membranes was occurred due to a greater molecular orientation and chain package. This had a great impact on membrane filtration performances where water permeability decreased while rejection increased with polymer concentration due to reduced membrane MWCO.

The effect of air gap length on the morphology and performance of PVDF hollow fiber membranes has been studied. The air gap lengths used were 1, 4, 11, and 15 cm.Based on AFM study, the membranes are not smooth. The nodule-like structure and nodule aggregates are formed on the outer surface of PVDF hollow fiber membranes. The surface nodule are aligned in direction of air gap length. The outer average nodule sizes of prepared membranes at air gap length of 1 cm was larger than the average nodule size of the hollow fiber prepared at >4 cm air

gap length. The roughness parameters decreased simultaneously with increasing the air gap length. Membrane water permeability was increased with increasing air gap length which was caused by decreasing the pore size and increasing the porosity of membranes. The results showed the PWP flux and suspended solid concentration in the permeate decreased by 43.65 % and 53.70 %, respectively, while porosity of hollow fiber membranes increased by 30 % with an increase of air gap length.

References

[1] H.I., Mahon, Permeability separatory apparatus and process using hollow fibers, U.S. Patent, 3,228,877 (1996b).

[3] L.Y. Yu, H.M. Shen, Z.L. Xu, PVDF-TiO_2 composite hollow fiber ultrafiltration membranes prepared by TiO_2 sol-gel method and blending method, J. Appl. Polym. Sci. 113 (2009) 1763-1772.

[4] A.F. Ismail, M.I.Mustaffar,R.M.Illias,M.S.Abdullah, Effect of dopeextrusionrate on morphology and performance of hollowfibermembranes for ultrafiltration,Sep. Purif. Technol.49 (2006) 10–19.

[5] S. Mok, D.J. Worsfold, A.E. Fouda, T. Matsuura, S. Wang, K. Chan, Study on the effect of spinning conditions and surface treatment on the geometry and performance of polymeric hollow-fibre membranes,J. Membr. Sci. 100 (1995) 183-192.

[6] T.S. Chung, J.J. Qin, J.Gu, Effect of shear rate within the spinneret on morphology, separationperformance and mechanicalproperties of ultrafiltrationpolyethersulfonehollowfibermembranes,J. Chem. Eng. Sci. 55 (2000) 1077-1091.

[7] G. Bakeri, A.F. Ismail, D. Rana, T. Matsuura, M. Shariaty, Investigation on the effects of fabrication parameters on the structure and properties of surface-modified membranes using response surface methodology, J. Appl. Polym. Sci. 123 (2012) 2812-2827.

[8] T.S. Chung, E.R. Kafchinski, The effects of spinning conditions on asymmetric 6FDA/ 6FDAM polyimide hollow fibers for air separation, J. Appl. Polym Sci. 66 (1997) 1555-1569.

[9] T.S. Chung, X. Hu, Effect of air gap distance on the morphology and thermal properties of the polyethersulfone hollow fibers, J. Appl. Polym. Sci. 66 (1997) 1067-1077.

[10] P. Aptel, N. Abidine, F. Ivaldi, J.P.Lafaille,Polysulfone hollow fibers-effect of spinning conditions on ultrafiltration properties,J. Membr. Sci. 22 (1985) 199-215.

[11] K.J. Kim, A.G. Fane, C.J.D. Fell, D.C. Joy, Fouling mechanisms of membranes during proteinultrafiltration,J. Membr. Sci. 68 (1995) 79-91.

[12] M. Khayet, The effects of air gap length on the internal and external morphology of hollow fiber membranes, Chem. Eng. Sci. 58 (2003) 3091-3104.

[13] D. Wang, K. Li, W. K.Teo, Porous PVDF asymmetric hollowfibermembranesprepared with the use small molecularadditives, J. Membr. Sci. 178 (1999) 13-23.

[14] N.H.A. Tsai, D.H. Huang, S.C. Fan, Y.C. Yang, C.L. Li, K.R. Lee, J.Y. Lai, Investigation of surfactantadditioneffect on the vapourpermeation of aqueousethanolmixtures through polysulfonehollow fiber membranes,J. Membr. Sci. 198 (2002) 245-258.

[15] K.C. Khulbe, C.Y.Feng, F.Hamad, T. Matsuura, M.Khayet, Structural and performancestudy of microporouspolyetherimidehollowfibermembranesprepared at differentairgap,J. Membr. Sci. 245 (2004) 191-198.

16. E. Yuliwati, A.F. Ismail, T. Matsuura, M.A. Kassim, M.S. Abdullah, Characterization of surface-modified porous PVDF hollow fibers for refinery wastewater treatment using microscopic observation, Desalination 283 (2011) 206-213.

16. M. Khayet, T. Matsuura,Preparation and characterization of polyvinylidenefluoridemembranes for membranedistillation, Ind. Eng. Chem. Res. 40 (2001) 5710-5718.

[17] J. Qin, J. Gu, T.S. Chung, Effect of wet and dry-jet wet spinning on the shear-induced orientation during the formation of ultrafiltration hollow fiber membranes, J. Membr. Sci. 182 (2001) 57-75.

[18] A.F. Ismail, A.R. Hassan, Formation and characterization of asymmetric nanofiltration membrane: Effect of shear rate and polymer concentration,J. Membr. Sci. 270(1-2) (2006) 57-72.

[19] E. Yuliwati, A.F. Ismail, Effect of additives concentration on the surface properties and performance of PVDF ultrafiltration membranes for refinery wastewater treatment, Desalination237 (2011) 226-234.

[20] E. Yuliwati, A.F. Ismail, T. Matsuura, M.A. Kassim, M.S. Abdullah, Characterization of surface-modified porous PVDF hollow fibers for refinery wastewater treatment using microscopic observation, Desalination (2011), In press.

[18] M. Khayet, C.Y. Feng, K.C. Khulbe, T. Matsuura, Preparation and characterization of polyvynilidene fluoride hollow fiber membranes for ultrafiltration, Polymer. 43 (2002) 1917-1935.

[19] G. Singh, I. Song, H. Li, Cake Compressible of Silica Colloids in Membrane Filtration Processess, Ind. Eng. Chem. Res. 54 (2008) 4023-4030.

[20] T.S. Chung, J.J. Qin, A.Huan, K.C. Toh, Visualization of the effect of dieshear rate on the outersurfacemorphology of ultrafiltrationmembranes by AFM,J. Membr. Sci. 196 (2002) 251-266.

[21] D.B. Mosqueda-Jimenez, R.M. Narbaitz, T. Matsuura, G.Chowdhury, G.Pleizier, J.P. Santerre, Influence of processingconditions on the properties of ultrafiltrationmembranes,J. Membr. Sci. 231 (2004) 209-224.

[22] C. Barth, M.C. Gonçalves, A.T.N. Pires, J. Roeders, B.A. Wolf, Asymmetric polysulfone and polyethersulfone membranes: Effects of thermodynamic conditions during formation on their performance,J. Membr. Sci. 169 (2000) 287-299.

[23] P. Lipp, C.H. Lee, A.G.Fane ,C.J.D. Fell, A fundamentalstudy of the ultrafiltration of oil-water emulsions,J. Membr. Sci. 36 (1988) 161-177.

[24] J. Qin, J. Gu, T.S. Chung, Effect of wet and dry-jet wet spinning on the shear-induced orientation during the formation of ultrafiltration hollow fiber membranes, J. Membr. Sci. 182 (2001) 57-75.

[25] N.H.A. Tsai, D.H. Huang, S.C. Fan, Y.C. Yang, C.L. Li, K.R. Lee, J.Y. Lai, Investigation of surfactantadditioneffect on the vapourpermeation of aqueousethanolmixtures through polysulfonehollow fiber membranes,J. Membr. Sci. 198 (2002) 245-258.

Polyvinylidene Fluoride Hollow Fiber Membranes for Refinery Wastewater Treatment: Effect of Air Gap Length on Membrane Morphology and Performance

ORIGINALITY REPORT

51%
SIMILARITY INDEX

PRIMARY SOURCES

1	M Khayet. "The effects of air gap length on the internal and external morphology of hollow fiber membranes", Chemical Engineering Science, 2003 Crossref	1053 words — 19%
2	E. Yuliwati, A.F. Ismail. "Effect of additives concentration on the surface properties and performance of PVDF ultrafiltration membranes for refinery produced wastewater treatment", Desalination, 2011 Crossref	846 words — 15%
3	E. Yuliwati, A.F. Ismail, T. Matsuura, M.A. Kassim, M.S. Abdullah. "Characterization of surface-modified porous PVDF hollow fibers for refinery wastewater treatment using microscopic observation", Desalination, 2011 Crossref	222 words — 4%
4	Yuliwati, E.. "Characterization of surface-modified porous PVDF hollow fibers for refinery wastewater treatment using microscopic observation", Desalination, 20111201 Crossref	131 words — 2%
5	Yuliwati, E.. "Effect of additives concentration on the surface properties and performance of PVDF	119 words — 2%

ultrafiltration membranes for refinery produced wastewater treatment", Desalination, 20110601
Crossref

6 N.A.A. Hamid, A.F. Ismail, T. Matsuura, A.W. Zularisam, W.J. Lau, E. Yuliwati, M.S. Abdullah. "Morphological and separation performance study of polysulfone/titanium dioxide (PSF/TiO2) ultrafiltration membranes for humic acid removal", Desalination, 2011 — 93 words — 2%
Crossref

7 M. Khayet, M.C. García-Payo, F.A. Qusay, M.A. Zubaidy. "Structural and performance studies of poly(vinyl chloride) hollow fiber membranes prepared at different air gap lengths", Journal of Membrane Science, 2009 — 86 words — 2%
Crossref

8 K. C. Khulbe, C. Y. Feng, T. Matsuura, D. C. Mosqueada-Jimenaez, M. Rafat, D. Kingston, R. M. Narbaitz, M. Khayet. "Characterization of surface-modified hollow fiber polyethersulfone membranes prepared at different air gaps", Journal of Applied Polymer Science, 2007 — 77 words — 1%
Crossref

9 Khayet, M.. "The effects of air gap length on the internal and external morphology of hollow fiber membranes", Chemical Engineering Science, 200307 — 40 words — 1%
Crossref

10 Woei-Jye Lau, A.F. Ismail. "Effect of SPEEK content on the morphological and electrical properties of PES/SPEEK blend nanofiltration membranes", Desalination, 2009 — 39 words — 1%
Crossref

11 Khayet, M.. "Effects of gas gap type on structural morphology and performance of hollow fibers", Journal of Membrane Science, 20080320 — 37 words — 1%

Crossref

12 E. Yuliwati, A.F. Ismail, T. Matsuura, M.A. Kassim, M.S. Abdullah. "Effect of modified PVDF hollow fiber submerged ultrafiltration membrane for refinery wastewater treatment", Desalination, 2011 — 33 words — 1%
Crossref

13 Tasselli, F.. "Tuning of hollow fiber membrane properties using different bore fluids", Journal of Membrane Science, 20070901 — 31 words — 1%
Crossref

14 Yadong Tang, Na Li, Anjun Liu, Shukai Ding, Chunhai Yi, Hao Liu. "Effect of spinning conditions on the structure and performance of hydrophobic PVDF hollow fiber membranes for membrane distillation", Desalination, 2012 — 31 words — 1%
Crossref

EXCLUDE QUOTES	OFF	EXCLUDE SOURCES	< 1%
EXCLUDE BIBLIOGRAPHY	ON	EXCLUDE MATCHES	OFF